PHYSICAL REVIEW B **90**, 241412(R) (2014)

Local control of the excitation of surface plasmon polaritons by near-field magneto-optical Kerr effect

R. Vincent,[1,*] H. Marinchio,[2] J. J. Sáenz,[3,4] and R. Carminati[2]

[1]*Laboratoire de Nanotechnologies et d'Instrumentation Optique, Institut Charles Delaunay, CNRS, Université de Technologie de Troyes, 12 Rue Marie Curie, F-10004 Troyes, France*

[2]*ESPCI ParisTech, PSL Research University, CNRS, Institut Langevin, 1 rue Jussieu, F-75005 Paris, France*

[3]*Condensed Matter Physics Center (IFIMAC), Departamento de Física de la Materia Condensada and Instituto "Nicolás Cabrera," Universidad Autónoma de Madrid, E-28049 Madrid, Spain*

[4]*Donostia International Physics Center (DIPC), Paseo Manuel Lardizabal 4, E-20018 Donostia-San Sebastian, Spain*

(Received 31 July 2014; revised manuscript received 25 November 2014; published 11 December 2014)

We investigate local control of the excitation of surface plasmon polaritons by a magnetic scatterer placed in the vicinity of a metallic surface. We show that under those conditions a change of about 27% in the surface plasmon intensity can be achieved by flipping the external magnetic field. The magnitude of this phenomenon is given by the magneto-optical Kerr effect (MOKE). A qualitative analysis of our numerical results, based on a perturbative approach, lead to simple analytical expressions for the longitudinal MOKE when the scatter is in close proximity to the surface. These results provide physical insight into the problem and may lead to the design of useful devices.

DOI: 10.1103/PhysRevB.90.241412 PACS number(s): 73.20.Mf, 78.20.Ls

Current interest in the magnetic properties of light at the nanoscale has been motivated by recent advances on the control of magnetic processes with ultrafast optics [1] and plasmonics [2]. Plasmonic research has focused so far on its potential for the design of elements for integrated and nanophotonic circuits, due to their possible applications in the industry. Magnetoplasmonics has emerged in response to the demand for an active element in such devices, through hybrid metal-ferromagnet structures [3]. Besides the application that we have mentioned, there are other aspects that make magnetoplasmonics an attractive area of research. Regarding this, we can mention the acceleration of magnetization reversal [4], amplification of the magneto-optical Kerr effect (MOKE) [5–7], and a higher density of magnetic recording [8]. We have recently explored the possibility of tuning the fluorescence resonance energy transfer (FRET) of a donor-acceptor couple in the vicinity of a magnetic particle by using the magnetic field as an external control parameter. The maximum effect was obtained in a near-field approximation [9].

In this Rapid Communication, we describe a magneto-plasmonic effect with interesting potential applications. The system considered is a magnetic scatterer at a subwavelength distance above a metallic surface and illuminated by a polarized light (see Fig. 1). The scatterer's magnetization can be oriented under an external static magnetic field, which can then be used to control the coupling between the incoming light and the surface plasmons through MOKE. Although the photons do not interact directly with the spin, the magnetic materials can affect the light, the origin of the interaction lying in the spin-orbit coupling between the spins and the electron orbitals [10,11]. This explains why the observed effect is weak. Different far-field detection schemes have been developed depending on the relative orientation of the light field and the local magnetization [3]. However, the spatial distribution of the MOKE signal still needs to be discussed in detail.

Here we focus on the so-called longitudinal MOKE configuration (LMOKE), i.e., when the magnetization is set parallel to both the reflection surface and the plane of incidence (x direction). As a concept, in order to analyze the magnetoplasmonic response, we introduce the spatial LMOKE signal $\eta(\mathbf{r})$, defined as

$$\eta \equiv [I(+\boldsymbol{M}) - I(-\boldsymbol{M})]/[I(+\boldsymbol{M}) + I(-\boldsymbol{M})], \qquad (1)$$

where $\boldsymbol{M}$ stands for the magnetization vector of the sample and $I(\mathbf{r},\pm\boldsymbol{M})$ is the scattered light intensity at a position $\mathbf{r}$. Based on the analysis of $\eta(\mathbf{r})$, we predict an enhancement of the MOKE at evanescent distances from the surface compared to its far-field value. Our study allows us to attribute this amplification to the surface plasmon polariton (SPP) contribution, demonstrating that the excitation of surface plasmon polaritons can be controlled by the external magnetic field, and also to define a quantity of interest for the system called the surface plasmon polariton magneto-optical Kerr effect (SPP-MOKE).

Our study is based on an extended discrete dipole approximation (DDA) and a Green's function method that we have used previously for the study of purely metallic structures [12,13]. We analyze the results based on our previous perturbative developments [14,15] where MO effects are introduced through an effective dielectric tensor $\boldsymbol{\epsilon}$ [16]. This tensor is controlled by the direction of magnetization, and the magnitude of the magneto-optical effect determined by the Voigt parameter Q, with the following expression,

$$\boldsymbol{\epsilon} = \epsilon \boldsymbol{I} + i\epsilon Q \boldsymbol{R} = \epsilon \begin{pmatrix} 1 & -iQM_z & iQM_y \\ iQM_z & 1 & -iQM_x \\ -iQM_y & iQM_x & 1 \end{pmatrix}, \qquad (2)$$

where Q is typically of the order of 10^{-3}–10^{-4} in the optical range. We consider the above-mentioned LMOKE configuration. Based on this, the light scattering calculation

*Corresponding author: remi.vincent@utt.fr

 ©2014 American Physical Society

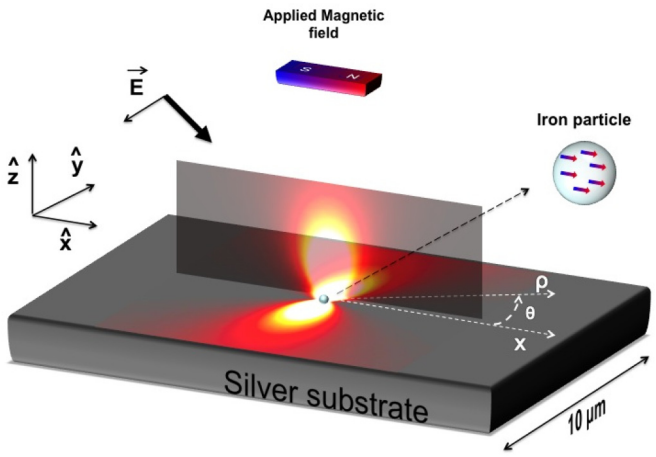

FIG. 1. (Color online) Calculation of the diffracted intensity of an s-polarized incident light ($\lambda = 800$ nm) over an iron nanoparticle at a distance of 10 nm of a silver substrate. The intensity is plotted in different cross sections of the space, xOy and xOy planes. The size of the iron nanoparticle (5 nm radius) is arbitrarily enhanced for illustration purposes, where the arrow illustrates the magnetization inside the nanoparticle, which is induced by the external magnetic field.

is treated as usual [12,17], directly replacing the scalar permittivity by its tensor counterpart $\boldsymbol{\chi}(\omega) = \boldsymbol{\epsilon}(\omega) - \mathbf{1}$. The magnetic scatter is discretized as a set of polarizable units [17,18], and the exact Green's function of a semi-infinite medium is used for the substrate [19].

Figure 1 is a representation of the scattered field intensity at a wavelength of 800 nm, for a nanoparticle of 5 nm radius, at a distance of 10 nm from the surface, with dielectric constants of silver extracted from Ref. [20], and for iron given by ellipsometric and polar Kerr spectra of thin iron films as in Refs. [21,22]. The cross sections presented in transparency clearly indicate two main scattering directions: the z direction, due to the far-field emission of the excited dipolar mode $\mathbf{p}_y$, and the y direction, due to the near-field coupling of the same induced dipole to the surface plasmon propagation mode.

From the diffracted field calculated for opposite directions of the magnetic field, we compute the MOKE for different spatial cross sections and obtain Figs. 2 and 3. These results reveal a high directivity (cf. Fig. 2), together with an enhancement in the proximity of the metallic substrate (cf. Fig. 3), which reaches the extraordinary magnitude of 27% for a polar angle of $\theta = 2.7^\circ$ with the x axis (for a distance to the substrate of 20 nm). This predicted amplitude is several times larger than the MOKE measurements reported so far [23–26]. At this point it is important to notice that we are considering the scattering field only, as it is experimentally possible to isolate this part by measuring the field away from the laser spot localized on the particle.

To explain the phenomenon at the origin of this effect, we use a perturbative formalism developed previously [14,15]. First, we consider a magnetic scatterer small enough to be treated as an electric dipole, and calculate the dipole moment $\mathbf{p}$ induced by the exciting field $\mathbf{E}_0$ at its position. This moment is expressed as follows,

$$\mathbf{p} = \epsilon_0 \boldsymbol{\alpha}_{\text{eff}} \mathbf{E}_0 = \mathbf{p}_I + \mathbf{p}_{\text{MO}} = \epsilon_0 (\boldsymbol{\alpha}_I + \boldsymbol{\alpha}_{\text{MO}}) \mathbf{E}_0, \qquad (3)$$

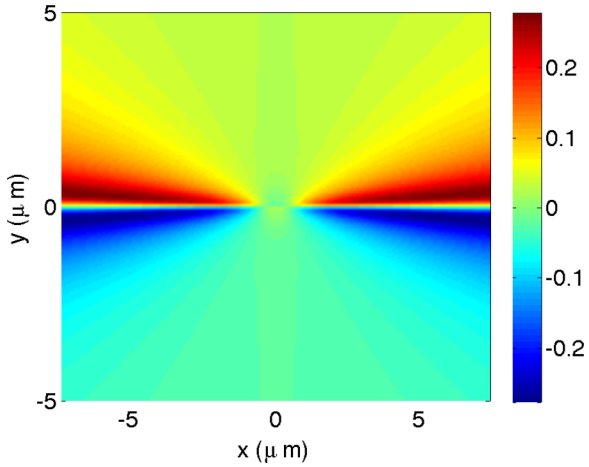

FIG. 2. (Color online) Cross section of the LMOKE diffracted intensity in the xOy plane, at a distance of 20 nm above the silver substrate, for the geometry and condition depicted in the caption of Fig. 1.

where $\boldsymbol{\alpha}_I$, $\boldsymbol{\alpha}_{\text{MO}}$ are respectively the diagonal component and the off-diagonal component of the effective polarizability tensor $\boldsymbol{\alpha}_{\text{eff}}$. In the previous expression, we consider that the polarizability is weakly affected by the presence of the substrate, which is valid in the limit of small particles with strong absorption [27]. Thus, by simplifying the effective polarizability tensor to its free-space expression, which includes the radiation reaction in vacuum, it is written as follows,

$$\boldsymbol{\alpha}_{\text{eff}} = \boldsymbol{\alpha}_0 \left(\mathbf{I} - \frac{ik^3}{6\pi} \boldsymbol{\alpha}_0 \right)^{-1}, \qquad (4)$$

where $\boldsymbol{\alpha}_0 = 3V(\boldsymbol{\epsilon} - \mathbf{1})(\boldsymbol{\epsilon} + \mathbf{2})^{-1}$ stands for the static polarizability, and $k = 2\pi/\lambda$ is the wave vector in vacuum.

The scattered field $\mathbf{E}^s(\mathbf{r})$ at a position $\mathbf{r}$ is therefore described with the Green's propagator as follows: $\mathbf{E}^s(\mathbf{r}) = \mu_0 \omega^2 \mathbf{G}(\mathbf{r}, \mathbf{r}')\mathbf{p}$. Furthermore, at far distances from the nanoparticle, and in proximity to the surface, the Green's tensor can be

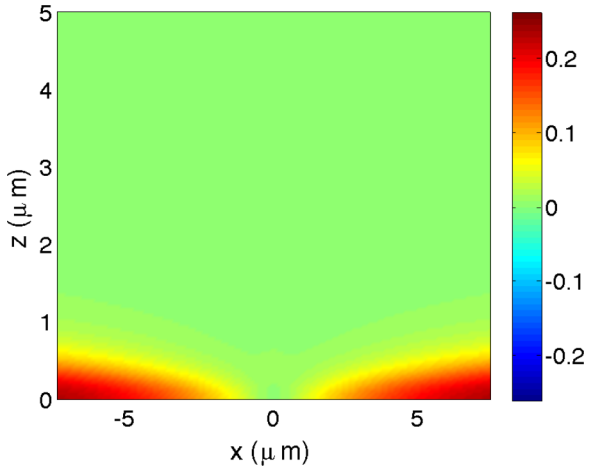

FIG. 3. (Color online) Cross section of the LMOKE diffracted intensity in the xOz plane, with $y = 500$ nm, for the geometry and condition depicted in the caption of Fig. 1.

reduced to its surface plasmon polariton part [28,29], which is given in cylindrical coordinates by the following expression,

$$\mathbf{G}_{\mathrm{SPP}}(\mathbf{r},\mathbf{r}') = \xi(\rho,z)\hat{\mathbf{u}}\hat{\mathbf{u}}^{\dagger}, \tag{5}$$

where $\hat{\mathbf{u}} = \frac{1}{(1+1/N^2)^{1/2}}(\frac{\hat{\boldsymbol{\rho}}}{N} + \hat{\mathbf{z}})$ is the unit vector of the SPP electric field, $\hat{\mathbf{u}}^{\dagger}$ the adjoint vector, N the refractive index of the substrate, $\hat{\boldsymbol{\rho}}$ the radial unit vector in cylindrical coordinates, and $\xi(\rho,z)$ a given analytical scalar function which can be easily obtained from Ref. [29]. Therefore, and according to the above expressions, in a region close to the surface but distant from the nanoparticle, the scattered electric field by the s-polarized plane wave over the magnetic particle can be written as follows,

$$\mathbf{E}^{s}(\mathbf{r}) \approx \mathbf{E}^{s}_{\mathrm{SPP}}(\mathbf{r}) \approx \xi(\rho,z)E_0\alpha_{yy}\left(\frac{\hat{\boldsymbol{\rho}}.\hat{\mathbf{y}}}{N} + \phi_{(+M_x)}\right)\hat{\mathbf{u}}, \tag{6}$$

where $\phi_{(+M_x)}$ is the complex Kerr rotation of the nanoparticle, with $\phi_{(+M_x)} = \arctan(\frac{\alpha_{yz}}{\alpha_{yy}}) \approx \frac{\alpha_{yz}}{\alpha_{yy}} \approx \frac{3i\epsilon Q}{(\epsilon+2)(\epsilon-1)}$ [15,30,31].

From Eqs. (1) and (6), we express the MOKE signal in proximity to the surface and far from the nanoparticle and obtain the following expression,

$$\eta(\theta) \approx \eta_{\mathrm{SPP}}(\theta) \approx \frac{|\sin\theta + N\phi|^2 - |\sin\theta - N\phi|^2}{|\sin\theta + N\phi|^2 + |\sin\theta - N\phi|^2}. \tag{7}$$

As this MOKE signal has been perturbatively obtained using the SPP field only in the propagating part, it has been denoted by the SPP-MOKE signal η_{SPP}. Given that the exciting field disappears from the previous expression, let us notice that the incidence angle has no effect on the MOKE.

Therefore, Eqs. (6) and (7) allow us to understand the MOKE of the scattered field in proximity to the surface resulting from the interference pattern of the two components of the surface plasmon polariton fields $\mathbf{E}^{s}_{\mathrm{SPP}}(\mathbf{r}) = \mathbf{E}^{s,I}_{\mathrm{SPP}}(\mathbf{r}) + \mathbf{E}^{s,\mathrm{MO}}_{\mathrm{SPP}}(\mathbf{r},M)$. Figure 4 is an illustration of the constructive-destructive effect depending on the magnetization direction, noting the antisymmetric property of the MO-SSP field as a function of the magnetization direction, $\mathbf{E}^{s,\mathrm{MO}}_{\mathrm{SPP}}(\mathbf{r},-M) = -\mathbf{E}^{s,\mathrm{MO}}_{\mathrm{SPP}}(\mathbf{r},M)$, which reveals the active part of the nanoantenna.

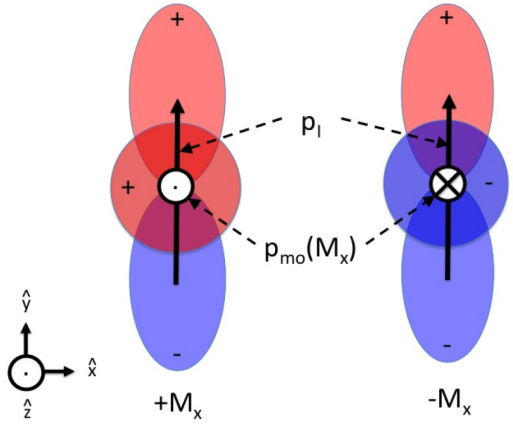

FIG. 4. (Color online) Schematic view of the directivity of the SPP far fields excited by the induced dipoles vs the directions of the magnetization. The induced dipoles and SPP fields are respectively decomposed in magneto-optical and dielectric parts. The colors illustrate the relative phases.

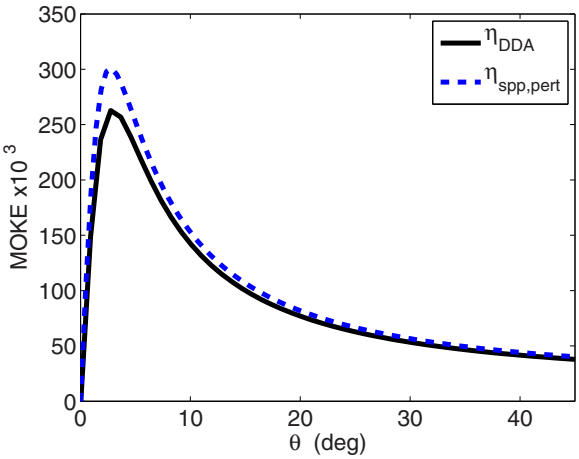

FIG. 5. (Color online) Comparison of the extended DDA results $\eta(\lambda = 800\ \mathrm{nm})$ at $\rho = 5\ \mu$m, $z = 20$ nm (solid black line), and the perturbative expression based on Eq. (3) (dashed blue line) as a function of the polar angle θ.

In Figs. 5 and 6, the SPP-MOKE contrast η_{SPP}, given by Eq. (7), is plotted together with the DDA-based calculation η_{DDA}. Their comparison shows a qualitative and quantitative agreement, i.e., between the numerical simulation and the SPP perturbative approach, confirming the SPP origin of the MOKE in proximity to the substrate. Furthermore, the analysis of Eq. (7) allows us to derive an expression for the polar angle $\theta = \cos\arg(N\phi)$ for which the MOKE parameter is maximum and equal to $\eta = \arcsin|N\phi|$, which is compatible with the DDA calculation. For instance, from Fig. 2, for the maximum MOKE, the model confirms a difference close to 27% (i.e., 30%) in SPP intensity between opposite directions of magnetization.

Considering the spectral dependency of $\eta(\lambda)$ along the y direction ($\theta = \pi/2$), plotted in Fig. 6, a simple development from Eq. (7) leads to a reduced expression as follows,

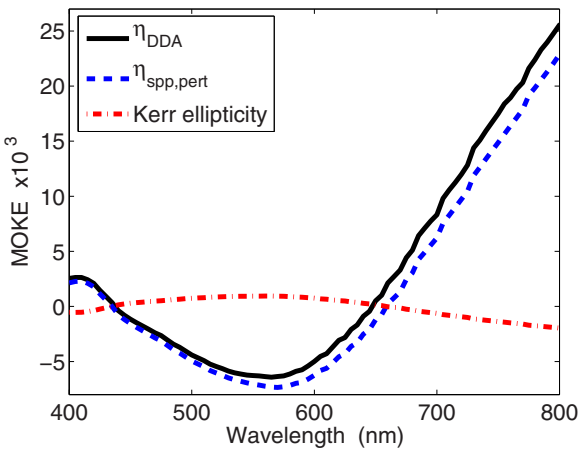

FIG. 6. (Color online) Comparison of the extended DDA results η in the y direction, at $\rho = 5\ \mu$m, $z = 20$ nm as the solid black line, the perturbative expression $-2N''\varphi$ as the dashed blue line, and the elliptic Kerr rotation φ as the dashed-dotted red line.

$\eta(\lambda) \approx -2N''(\lambda)\varphi(\lambda)$, where $\varphi = \mathrm{Im}(\phi)$ is the nanoparticle elliptic Kerr rotation and N'' the imaginary part of the substrate refractive index. The elliptical Kerr rotation, plotted in this same figure, shows that the qualitative behavior of the SPP-LMOKE in this direction results from the elliptical Kerr rotation, whereas the enhancement, compared to the MOKE far from the substrate, results from the anisotropic excitation of the SPP field (cf. the $\hat{\mathbf{u}}$ vector). Even in the direction of the weakest signal, a modulation of a few percent is achievable. This slight imbalance reflects the directivity control along the y axis. From this case study, it is worth noticing that adding a geometric anisotropy to the particle could bring a larger control in the directivity of the nanoantenna.

In conclusion, we have demonstrated theoretically a method to control the SPP excitation through the Kerr effect. An up to 27% of change in the intensity of the SPP is reached in a given direction. A measurement of this effect is realizable simply by leakage radiation microscopy. Finally, an analytical expression to explain the feature of the local control of the excitation of surface plasmon polaritons by the near-field magneto-optical Kerr effect has been derived. Furthermore, due to the separate origin of the amplified MOKE signal given by the plasmon resonance [7], and our SPP-MOKE signal, one could expect a summation of the effects.

We would like to thank A. García-Martín for providing us with the experimental data on iron. This work was supported by the EU Project Nanomagma NMP3-SL-2008-214107, and LABEX ACTION (ANR-11-LABX-01-01) and the Spanish MINECO through FIS2012-36113. J.J.S. acknowledges support from an IKERBASQUE Visiting Fellowship.

[1] J.-Y. Bigot, M. Vomir, and E. Beaurepaire, Nat. Phys. **5**, 515 (2009).
[2] V. V. Temnov *et al.*, Nat. Photonics **4**, 107 (2010).
[3] G. Armelles, A. Cebollada, A. García-Martín, and M. Ujué-González, Adv. Opt. Mater. **1**, 2 (2013).
[4] L. Bogani *et al.*, Adv. Mater. **22**, 4054 (2010).
[5] E. Ferreiro-Vila, M. Iglesias, E. Paz, F. J. Palomares, F. Cebollada, J. M. González, G. Armelles, J. M. García-Martín, and A. Cebollada, Phys. Rev. B **83**, 205120 (2011).
[6] G. Armelles *et al.*, J. Opt. A: Pure Appl. Opt. **11**, 114023 (2009).
[7] P. K. Jain *et al.*, Nano Lett. **9**, 1644 (2009).
[8] B. C. Stipe *et al.*, Nat. Photonics **4**, 484 (2010).
[9] R. Vincent and R. Carminati, Phys. Rev. B **83**, 165426 (2011).
[10] H. R. Hulme, Proc. R. Soc. London, Ser. A **135**, 237 (1932).
[11] P. Bruno, Y. Suzuki, and C. Chappert, Phys. Rev. B **53**, 9214 (1996).
[12] C. Vandenbem, L. S. Froufe-Pérez, and R. Carminati, J. Opt. A: Pure Appl. Opt. **11**, 114007 (2009).
[13] C. Vandenbem, D. Brayer, L. S. Froufe-Pérez, and R. Carminati, Phys. Rev. B **81**, 085444 (2010).
[14] S. Albaladejo *et al.*, Opt. Express **18**, 3556 (2010).
[15] H. Marinchio, J. J. Sáenz, and R. Carminati, Phys. Rev. B **85**, 245425 (2012).
[16] P. S. Pershan, J. Appl. Phys. **38**, 1482 (1967).
[17] L. S. Froufe-Perez and R. Carminati, Phys. Rev. B **78**, 125403 (2008).
[18] M. A. Yurkin and A. G. Hoekstra, J. Quant. Spectrosc. Radiat. Transfer **106**, 558 (2007).
[19] J. E. Sipe, J. Opt. Soc. Am. B **4**, 481 (1987).
[20] R. W. Christy, Phys. Rev. B **6**, 4370 (1972).
[21] E. Th. Papaioannou, V. Kapaklis, P. Patoka, M. Giersig, P. Fumagalli, A. Garcia-Martin, E. Ferreiro-Vila, and G. Ctistis, Phys. Rev. B **81**, 054424 (2010).
[22] B. Caballero, A. García-Martín, and J. C. Cuevas, Phys. Rev. B **85**, 245103 (2012).
[23] V. I. Belotelov *et al.*, Nat. Nanotechnol. **6**, 370 (2011).
[24] D. M. Newman *et al.*, J. Phys.: Condens. Matter **20**, 345230 (2008).
[25] C. Penfold, R. T. Collins, A. P. B. Tufaile, and Y. Souche, J. Magn. Magn. Mater. **242-245**, 964 (2002).
[26] S. Melle *et al.*, Appl. Phys. Lett. **83**, 4547 (2003).
[27] A. B. Evlyukhin, G. Brucoli, L. Martín-Moreno, S. I. Bozhevolnyi, and F. J. García-Vidal, Phys. Rev. B **76**, 075426 (2007).
[28] T. Søndergaard and S. I. Bozhevolnyi, Phys. Rev. B **67**, 165405 (2003).
[29] T. Søndergaard and S. I. Bozhevolnyi, Phys. Rev. B **69**, 045422 (2004).
[30] J. B. Gonzalez-Diaz *et al.*, Appl. Phys. Lett. **97**, 043114 (2010).
[31] B. Sepulveda, J. B. González-Díaz, A. García-Martín, L. M. Lechuga, and G. Armelles, Phys. Rev. Lett. **104**, 147401 (2010).